SSRG International Journal of Electrical and Electronics Engineering
ISSN: 2348-8379/ https://doi.org/10.14445/23488379/IJEEE-V12I11P105

Volume 12 Issue 11, 48-57, November 2025

Original Article

A Probabilistic Evaluation of the Reliability of a 1 MWP Solar Power Plant With String Topology: a Case Study in Arequipa, Peru.

Wilson Omar Ramos Parqui[1], Luis Felipe Florez Mollepaza[2], German Alberto Echaiz Espinoza[3]

[1,2,3]*Universidad Nacional de San Agustin de Arequipa, Arequipa, Perú*

[1]*Corresponding Author : wramospa@unsa.edu.pe*

Received: 04 September 2025 Revised: 06 October 2025 Accepted: 05 November 2025 Published: 28 November 2025

Abstract *- Photovoltaic systems require reliability assessments to ensure continuous energy availability. This study assesses the reliability of a 1 MWp centralized photovoltaic plant with a string topology using a probabilistic approach based on Markov chains, which incorporates component failure and repair rates. Real hourly irradiance data from Arequipa, one of the regions with the highest solar incidence in South America, were modeled using a Probability Mass Function (PMF). The analysis included the Capacity Outage Probability Table (COPT) and the impact of the inverter's minimum DC input voltage on system availability. The results obtained were ISE = 2,277.02 MWh, ESE = 2,179.95 MWh, and Ae = 0.9573 for the evaluated period, indicating high energy reliability of the photovoltaic plant.*

Keywords *- Reliability, Photovoltaic, Inverter, Copt, Ise, Ese, Ae.*

1. Introduction

Solar photovoltaic energy has grown rapidly worldwide due to the increase in installed capacity and the need to address issues that may affect system performance. Ensuring that a solar power plant maintains its expected electricity generation throughout its lifetime is essential for both technical and financial reasons [1]. Reliability [2], which is important in this context, is the likelihood that a system will perform its intended function within a specific period and under predefined conditions. It is necessary to evaluate the reliability of the system due to the intermittence and variability in energy availability. In addition, the high failure rate of components can directly affect the continuous energy supply.

In this way, it allows us to evaluate and plan maintenance and operation efficiently [3]. Several methodologies and criteria are used in the literature to assess the reliability of power generation systems. Among the primary methodologies employed are Markov models, Monte Carlo simulation, Fault Tree Analysis (FTA), and Failure Mode and Effects Analysis (FMEA). Likewise, criteria such as failure and repair rates are fundamental, as they enable the calculation of metrics such as Mean Time Between Failures (MTBF) and Mean Time To Repair (MTTR). With these data, whether from failure and repair records or parameters such as irradiance, it becomes possible to estimate reliability indices such as Loss of Load Expectation (LOLE), Loss of Load Probability (LOLP), among others [3, 4]. The reliability analysis of the system becomes more effective when performed at the component level, since the failure of an equipment can directly affect the energy supply. It is important to perform an individual evaluation of each component. When a module fails, the system can still supply energy through the remaining strings, but if an inverter or transformer fails, there is a possibility that the entire plant stops supplying energy [5-7].

Taking this into account, it is possible to identify the most critical components of the system and, therefore, plan the maintenance of this equipment in a more strategic manner. Studies assess system reliability based on energy availability, comparing the Ideal Generated Energy (ISE) with the Expected Generated Energy (ESE) during operation.

The analysis considers irradiance data and the failure and repair rates of system components, allowing a more accurate evaluation of the plant, since, by including irradiance, it is possible to estimate the energy availability of the system (Ae) even under variations of the solar resource [8]. In most studies, failure and repair rates are used without considering irradiance data, and in other cases, irradiance is included, but in a simplified way. Furthermore, a large part of the studies was conducted in temperate climate regions, which do not represent locations with high solar incidence. Therefore, it is important to evaluate reliability in high-irradiance regions, such as southern Peru, where studies that represent the real operating conditions of photovoltaic plants are still lacking.

2. Literature Review

Several studies have evaluated photovoltaic system reliability using different approaches. In [8], a reliability assessment for photovoltaic systems is conducted by comparing three inverter topologies: centralized, string, and multi-string. The analysis was carried out using the state enumeration method, considering the failure and repair rates of the system components. For the study, seasonal clustered irradiance was used, and the adopted reliability indicators were ISE, ESE, and Ae. Among the results presented, it was observed that the multi-string topology showed the highest availability with Ae = 0.9838, while the centralized topology was the least resilient, with Ae = 0.9735. The string topology presented a good performance balance, with Ae = 0.9807.

In [9], a 20 MWp photovoltaic plant with a string topology was analyzed, comparing two architectures: one using only series-connected strings and another combining series and parallel string configurations. A probabilistic method based on Markov chains and the Z-transform was developed to compute reliability.

The failure and repair rates were collected from the literature to construct the capacity state tables, resulting in an estimated availability of 83% for Architecture 1 and 88% for the second configuration. The analysis did not include irradiance data, considering only electrical failure and repair parameters. Similarly, [10], a photovoltaic power plant located in Agigea, Romania, with a capacity of 0.5 MWp, was analyzed using Markov chains to calculate reliability indices such as MTBF, MTTF, failure rates, and repair rates. For the analysis, failures recorded between February 2016 and December 2017 were considered. The results showed that, during the analyzed period, an average of one failure per year was observed, which could reach up to two or three failures per year. The maximum downtime was 1.8 hours. The method enabled the sizing of spare parts stock, thus avoiding unavailability. In the analysis, no irradiance or temperature data were considered, relying solely on failure and repair events.

Another contribution in [11] evaluated the reliability of components in large-scale photovoltaic plants by comparing central and string inverter topologies, aiming to quantify failure and repair rates and their impact on availability and energy losses. The analysis was performed through FTA and FMEA modeling. The data were obtained from real operational records, covering periods between 2 and 7 years, in plants ranging from 1.4 to 3.5 MWp. The findings indicated an energy availability of 98.37% for the central inverter topology and 99.07% for the string topology. Additionally, it was found that approximately two-thirds of total energy losses are associated with failures in inverters and transformers, highlighting the transformer as a critical component due to its high repair time. The study did not include irradiance data in the failure analysis.

In a different context, [12], a 100 MWp photovoltaic plant was analyzed for the assessment of composite reliability between generation and transmission. The model was developed using the COPAFT method, incorporating solar irradiance variability based on one year of hourly data from the Santa Maria, California region, while also accounting for component unavailability using failure and repair rates obtained from the literature. System reliability was evaluated through Monte Carlo simulation using state sampling.

The metrics used were LOLP, LOLF, LOLE, and the plant's equivalent capacity. The main results showed that the location of the photovoltaic plant directly influences the improvement of system reliability. In the case study applied to the IEEE RTS, buses 23, 2, 13, 16, and 18 showed the greatest positive impact on reliability indices.

A more component-focused assessment was conducted in the reliability of a 0.5 MWp photovoltaic plant with string topology was evaluated using hourly irradiance data from a region in southern Brazil. The analysis was performed through probabilistic modeling based on component failure and repair rates. Irradiance was treated using a Probability Mass Function (PMF), and system reliability was quantified using the COPT method to compute the ISE, ESE, and Ae indicators. The results showed high energy availability, Ae = 0.99996, and even with a 200% increase in failure rates, the system maintained high robustness, Ae = 0.99988.

Building upon these contributions, this study provides a more detailed reliability assessment at the component level, enabling a deeper evaluation of the individual and combined impact of PV modules, strings, inverters, and transformers. The irradiance dataset was obtained for Arequipa, Peru-one of the regions with the highest solar incidence in South America-ensuring a realistic representation of local operating conditions.

Failure and repair rates were compiled from the literature based on different photovoltaic plants, forming a more comprehensive and robust parameter base for probabilistic reliability modeling. This work also extends the study originally presented in, published in a conference, by incorporating real irradiance data and a more representative and diversified reliability parametrization.

3. Analysis Methodology

The topological configuration of a photovoltaic power plant directly influences the reliability of the system. Various configurations have been implemented, such as string, multi-string, and centralized topologies, which are among the most commonly used. Each presents its own advantages and disadvantages, as well as different costs and levels of system complexity. The appropriate choice of topology is crucial for ensuring system efficiency [6, 8, 13].

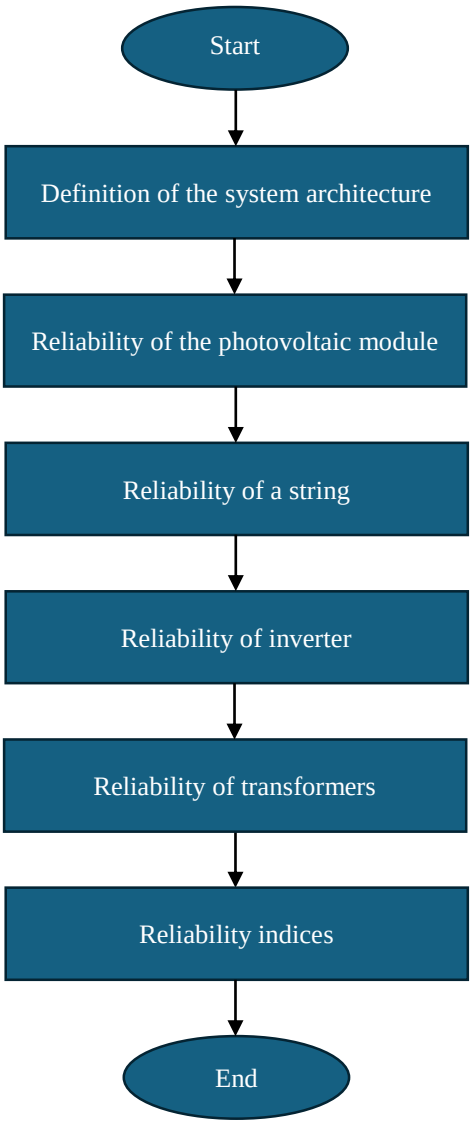

Fig. 1 Methodology for the Reliability Analysis

Figure 1 presents the flowchart used in the methodology, which guides the steps for system reliability evaluation and analysis. In this study, the string topology is employed, consisting of connecting photovoltaic modules in series to form a string, which is then connected to an inverter. Similarly, several strings are connected, each associated with its own inverter. This topology improves energy efficiency because, in the event of a photovoltaic module failure, the system continues to supply energy to the grid without compromising the entire plant's operation [13].

The selection of this topology is due to its combination of the advantages of microinverter systems, thanks to their simplicity, with those of centralized systems. The string topology is widely used in residential and commercial systems. In case of an inverter failure, only the associated string is affected, maintaining power generation in the rest of the plant. Furthermore, this topology presents lower power losses, contributing to a longer equipment lifespan [8, 13]. The reliability assessment of the photovoltaic plant is carried out sequentially, beginning with the analysis of the reliability of the photovoltaic modules, followed by the strings, and up to the transformer. The probability of operation or failure of each component is calculated using a probabilistic approach based on fundamental principles of probability theory [14]. This method provides a clear framework for application to each component, allowing the overall system reliability to be determined from the reliability of individual elements.

3.1. Reliability of the Photovoltaic Module

The analysis begins with the individual photovoltaic modules, each of which may supply energy (p_{fvc}) or may not supply energy (q_{fvc}). When a panel fails, it is isolated from the circuit by the bypass diode. The string current remains intact due to the series connection of the modules; however, a voltage drop occurs, resulting in a reduction of overall output power.

The operating and failure probabilities are given by:

$$p = \frac{\mu}{\mu+\lambda} \tag{1}$$

$$q = \frac{\lambda}{\lambda+\mu} \tag{2}$$

Each module is connected to the string through two MC4 connectors, which link the positive and negative terminals. Assuming independence between the events "module operates," "positive connector operates," and "negative connector operates," the probability that the module-connector set supplies energy is given by Equation (3).

$$p_{fvc} = P\left(p_{c^-}\middle|P\left(p_{fv}|p_{c^+}\right)\right) = p_{c^-} \cdot p_{fv} \cdot p_{c^+} \tag{3}$$

Where p_{fv} represents the operating probability of the module, p_{c^-} corresponds to that of the negative connector, p_{c^+} to that of the positive connector, and p_{fvc} denotes the probability that the combined module–connector set operates correctly.

The probability that the set does not supply energy to the string is complementary and is given by Equation (4).

$$q_{fvc} = 1 - p_{fvc} \tag{4}$$

3.2. Reliability of a String

Each photovoltaic panel can assume two states: supplying energy (p_{fvc}) or not supplying energy (q_{fvc}). When a panel fails, it is isolated from the circuit by the bypass diode. Since the modules are connected in series, the string current is not interrupted; however, a voltage reduction occurs, resulting in a decrease in total power.

The probability of the occurrence of a state $\beta(N_{fs})$, in which N_{fs} panels out of a total of N_S Are not operating, as given by Equation (5):

$$P\left(\beta(N_{fs})\right) = p_{fvc}^{N_S - N_{fs}} \cdot q_{fvc}^{N_{fs}} \quad (5)$$

Since different combinations of N_{fs} Panels may be inoperative, the exact probability of state $S(N_{fs})$ is given by Equation (6):

$$\begin{aligned} P(S(N_{fs})) &= \binom{N_S}{N_{fs}} P\left(\beta(N_{fs})\right) \\ &= \frac{N_S!}{N_{fs}!(N_S - N_{fs})!} P\left(\beta(N_{fs})\right) \end{aligned} \quad (6)$$

Where $\binom{N_S}{N_{fs}}$ represents the number of possible combinations of N_S panels taken N_{fs} at a time.

3.3. Reliability of Inverter

The operating (p_i) and failure (q_iProbabilities of an inverter are derived from its failure rate (λ_i) and repair rate (μ_i). In this configuration, each string is connected to a single inverter; therefore, a failure in the equipment results in the loss of all energy generated by that string.

An independent event producing the same effect is the failure of the DC switch that connects the string to the inverter. Consequently, the operating (p_{si}) and failure (q_{si}) probabilities of the inverter–DC switch set are defined by Equations (7), and (8):

$$\begin{aligned} p_{si} &= P(p_i | p_{s^{dc}}) \\ p_{si} &= p_i \cdot p_{s^{dc}} \end{aligned} \quad (7)$$

$$q_{si} = 1 - p_{si} \quad (8)$$

Considering that the inverters are connected in parallel, the probability $P\left(I(N_{fi})\right)$ that N_{fi} inverters out of a total of N_I The supply of energy is given by Equation (9):

$$P\left(I(N_{fi})\right) = \binom{N_I}{N_{fi}} p_{si}^{N_I - N_{fi}} \cdot q_{si}^{N_{fi}} \quad (9)$$

3.4. Reliability of Transformers

The reliability calculation for transformers follows the same procedure applied to inverters, also considering the presence of an AC switch that connects the equipment to the system. If the switch fails, the transformer is unable to supply energy to the grid. The operating (p_t) and failure (q_t) probabilities are derived from the failure rate (λ_t) and repair rate (μ_t). When multiple transformers are present, the probability that N_{ft} units, out of a set of N_T Simultaneously failing to supply energy is expressed by Equation (10):

$$P\left(T(N_{ft})\right) = \binom{N_T}{N_{ft}} p_{st}^{N_T - N_{ft}} \cdot q_{st}^{N_{ft}} \quad (10)$$

3.5. Reliability Indices

3.5.1. Ideal Supplied Energy

The ISE corresponds to the maximum amount of energy that could be delivered to the grid in a fully reliable system, that is, one without any component failures. Its calculation considers the available irradiance and the efficiency of the equipment, as expressed in Equation (11):

$$\text{ISE} = \sum_{k=1}^{K} E_{mk} P(E_{mk}) A_{fv} \eta_k N_S N_I \eta_i T_o \quad (11)$$

In this expression, E_{mk} represents the k-th irradiance value from the solar incidence probability distribution at the plant site, and $P(E_{mk})$ is the probability associated with that irradiance. Only nonzero irradiance values are considered in constructing this distribution. The area of each photovoltaic module is denoted by A_{fv}, while η_k corresponds to the module efficiency at the irradiance level E_{mk}. The number of modules per string is given by N_S, the number of inverters is N_I, represents the overall efficiency of the inverters. Finally, T_o s the total operating time during the analysed period.

3.5.2. Expected Supplied Energy

The ESE represents the amount of energy expected to be delivered to the power grid when considering the reliability of the plant components. Its calculation is more complex than that of the ISE and is therefore developed in stages.

The first stage involves evaluating the expected energy of a single string, denoted as, ESE_s. In this analysis, the minimum operating voltage of the inverter must be considered. When several modules in the exact string are disconnected due to failures, the voltage may drop below the minimum threshold. V_m, preventing the inverter from operating. In such cases, the energy generated by the remaining modules is also lost. Thus, ESE_s It is calculated according to Equation (12):

$$\text{ESE}_S = \sum_{s=0}^{N_S} \Gamma(V_s)(N_S - N_{fs}) P(S(N_{fs})) T_o \quad (12)$$

Here, s represents the number of failed modules, N_S the total number of modules per string, N_{fs} the number of failed modules, $P(S(N_{fs}))$ the probability of occurrence of the corresponding state, and T_o The operating time is considered. The function $\Gamma(V_s)$ defines the power delivered by the modules whenever the string voltage V_s is greater than or equal to the inverter's minimum voltage V_m, as defined in Equation (13):

$$\Gamma(V_s) = \begin{cases} \sum_{k=1}^{K} E_{mk} P(E_{mk}) A_{fv} \eta_k, & if\ V_s \geq V_m \\ 0, & \text{otherwise} \end{cases} \quad (13)$$

Once ESE_s is obtained, the expected supplied energy of all inverters, ESE_I, is calculated, also considering the failure probabilities of these devices. The calculation is expressed in Equation (14):

$$\mathrm{ESE}_I = \sum_{i=0}^{N_I} \mathrm{ESE}_S(N_I - N_{fi}) P\left(I(N_{fi})\right) \eta_i \qquad (14)$$

In the final stage, transformer reliability is incorporated into the analysis.

As transformers fail, the maximum power transferable by the remaining operational units decreases. Consequently, the global ESE is determined according to Equation (15):

$$\mathrm{ESE} = \sum_{t=0}^{N_T} T(P_{maxt})(N_T - N_{ft}) P\left(T(N_{ft})\right) \qquad (15)$$

Where N_T Is the total number of transformers, N_{ft} Is the number of failed units, $P(T(N_{ft}))$ represents the probability of the corresponding state, and P_{maxt} The maximum power that the transformers are capable of transmitting. The function $T(P_{maxt})$, defined in Equation (16), establishes the limit that ensures the available capacity is not exceeded.

$$T(P_{maxt}) = \begin{cases} \mathrm{ESE}_I, & if \ \ \mathrm{ESE}_I \le P_{maxt} \\ P_{maxt}, & \text{otherwise} \end{cases} \qquad (16)$$

3.5.3. Energy Availability

Energy availability (A_e) is the ratio between ESE and ISE, representing the portion of energy that the system is capable of delivering after accounting for possible equipment failures and their effects on the system. The calculation is presented in Equation (17).

$$A_e = \frac{\mathrm{ESE}}{\mathrm{ISE}} \qquad (17)$$

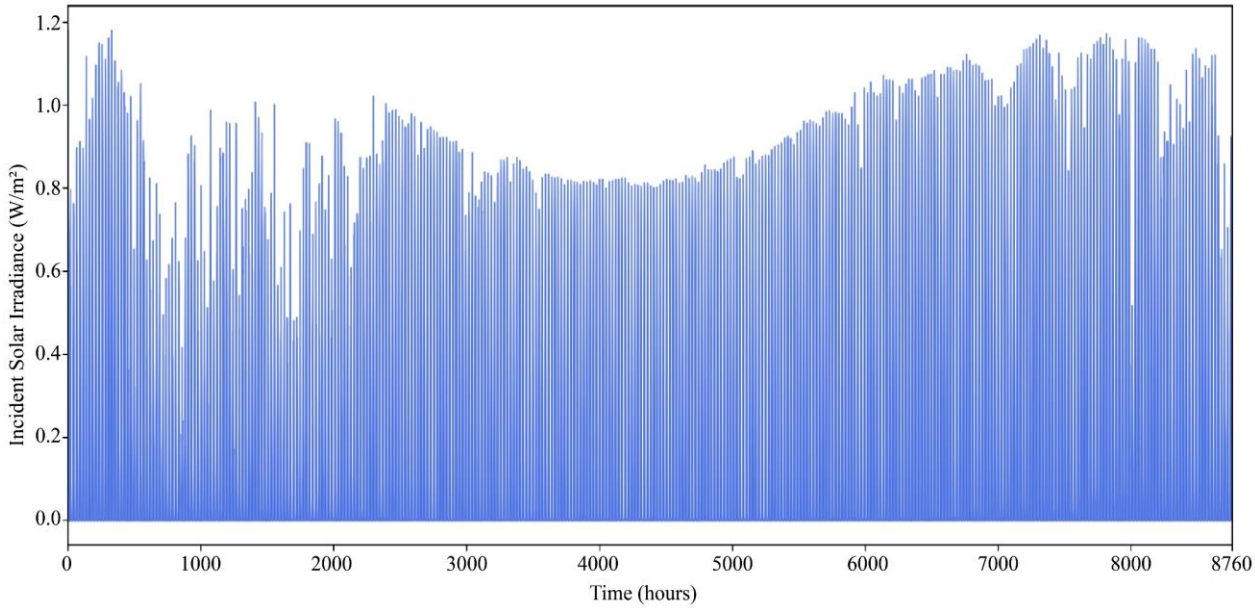

Fig. 2 Hourly solar irradiance profile

4. Case Study

This section presents a case study of a centralized photovoltaic power plant with an installed capacity of 1.0 Megawatt-Peak (MWp).

Figure 2 illustrates the topology of the adopted configuration, while Figure 3 presents the hourly irradiance profile over one year, obtained from the PVGIS tool (JRC-EU) [15]. For this analysis, the site was configured in Arequipa, Peru (16°24'43.2"S, 71°31'55.2"W), and data were collected for the entire year of 2023 with hourly resolution.The assessment of the plant is based on the failure and repair rates of each component, whose values were obtained from studies reported in the specialized literature, as shown in Table 1.

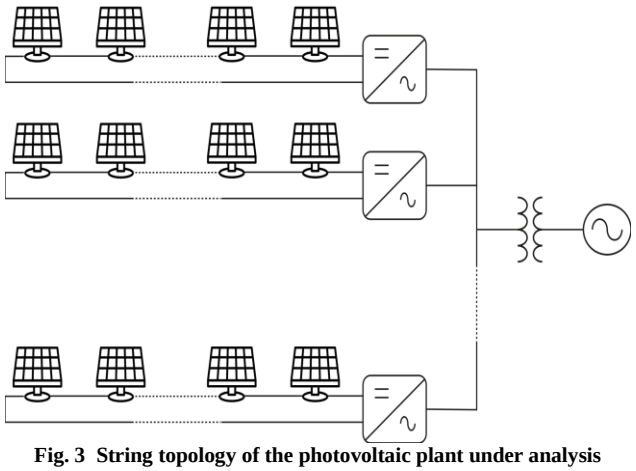

Fig. 3 String topology of the photovoltaic plant under analysis

Table 1. Failure and repair rates of components

Component	$\lambda\ [10^{-6}h^{-1}]$	$\mu\ [h^{-1}]$
PV Module	24 [16]	0.0039 [16]
Junction Box	14.269 [10]	1 [10]
Inverter	180 [17]	0.0057 [18]
DC Switch	0.2 [5, 19-21]	0.0208 [5, 19-21]
AC Switch	0.7 [17]	0.0208 [5, 19-21]
Bypass Diode	5.4 [5, 19-21]	0.0208 [5, 19-21]
Transformer	0.23 [10]	285.4 [10]

The characteristics of the photovoltaic modules and inverters considered in the analysis are presented in Tables 2 and 3. These characteristics were taken from real equipment in order to ensure greater accuracy and representativeness in the study.

Table 2. Technical specifications of photovoltaic modules

Module Efficiency	21.25	%
Maximum Power (Pmax)	650	W
Maximum Power Voltage (Vm)	36.79	V
Maximum Power Current (Im)	17.67	A
Height	2.384	m
Width	1.303	m

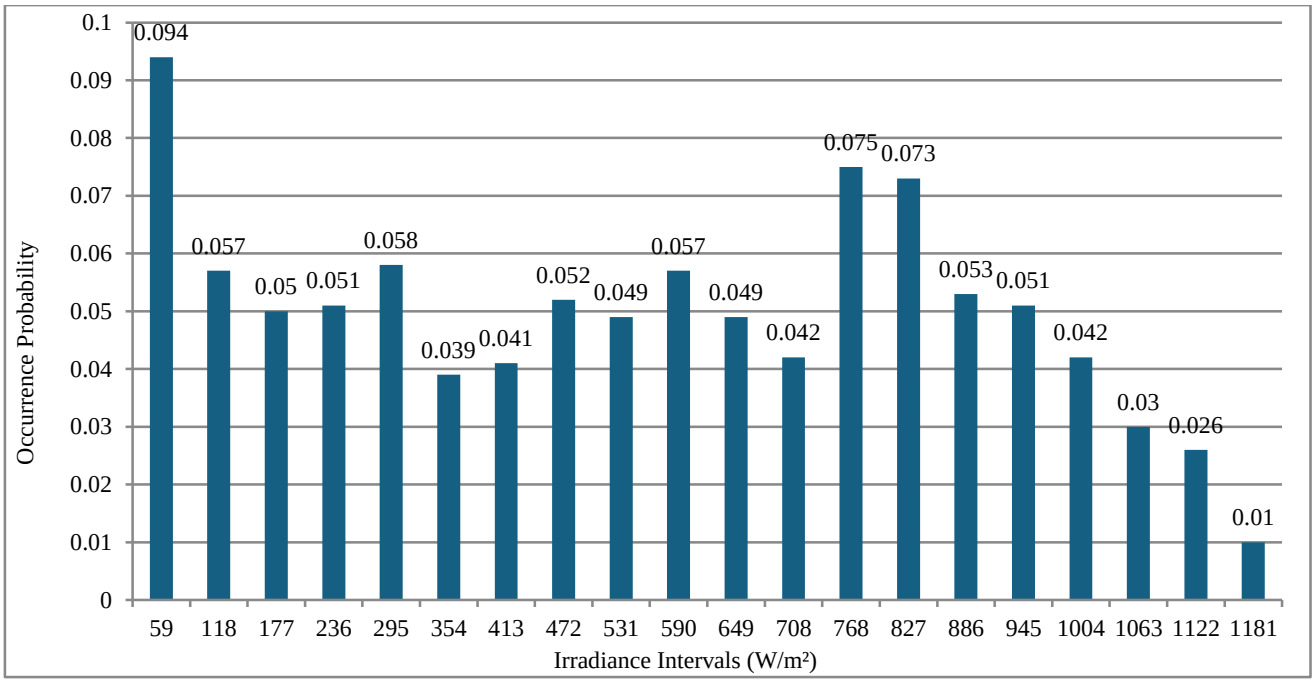

Fig. 4 Probability mass function of irradiance

Table 3. Technical specifications of inverters

Maximum Efficiency	99.02	%
Maximum DC Input Voltage	1100	V
Minimum Voltage	250	V
Nominal Voltage	580	V
Maximum DC Input Current per MPPT	32	A
Maximum AC Output Power	22000	W
Maximum AC Output Current	32	A

4.1. System Configuration

This dependability investigation utilized hourly irradiance data for a complete year, as depicted in Figure 3, amounting to 8760 records. The readings were categorized into twenty various ranges, omitting instances of zero irradiance. The Probability Mass Function (PMF) was generated using the frequency of occurrences within each range, as illustrated in Figure 4.

5. Results

Given the maximum inverter input voltage (V_{maxInv} = 1100 V) and the maximum voltage of the photovoltaic module (V_{maxPV} = 36.79 V), the number of panels per string is obtained by the relation:

$$\frac{V_{maxInv}}{V_{maxPV}} = N_{PV_s}$$

Therefore, each string consists of 29 panels.

The inverter's nominal capacity is 22 kW, yet each string only has 18.85 kW of electricity. For a 1.0 MWp system, you need 52 inverters. The average irradiance of 526.58 W/m² and the probability in Table 1 were used to figure out the system's ISE and ESE values. To improve the study of nominal power, the time fraction T_o Was left out of the Capacity Outage Probability Table (COPT) intermediate calculations and only included in the final result. Table 4 presents the values of

P_{ideal_S} and $P_{expected_S}$ for the solar panels. Similarly, Tables 5 and 6 present the results for transformers and inverters. The probability distribution consistently highlights conditions of low unavailability, resulting in minor deviations between ideal and projected power outputs. With the values of P_{ideal_T} and $P_{expected_T}$ it is possible to obtain the ISE values: 2,277.02 MWh and ESSE: 2,179.95 MWh. Using Equation (17), Ae = 0.9573 is obtained, which corresponds to 95.73% of the effective energy delivered to the power grid, indicating high system reliability.

Table 4. COPT of PV modules

N_{fs}	Ideal Power (W)	Probability	Expected Power (W)
0	10080.27	8.36E-01	8.379E+03
1	9732.67	1.50E-01	1.450E+03
2	9385.08	1.30E-02	1.211E+02
3	9037.48	7.22E-04	6.487E+00
4	8689.89	2.90E-05	2.506E-01
5	8342.29	8.97E-07	7.438E-03
6	7994.7	2.22E-08	1.763E-04
7	7647.1	4.51E-10	3.425E-06
8	7299.51	7.66E-12	5.559E-08
9	6951.91	1.11E-13	7.638E-10
10	6604.31	1.37E-15	8.972E-12
11	6256.72	1.46E-17	9.077E-14
12	5909.12	1.35E-19	7.950E-16
13	5561.53	1.09E-21	6.049E-18
14	5213.93	7.73E-24	4.007E-20
15	4866.34	4.78E-26	2.312E-22
16	4518.74	2.59E-28	1.162E-24
17	4171.15	1.22E-30	5.069E-27
18	3823.55	5.04E-33	1.915E-29
19	3475.96	1.80E-35	6.232E-32
20	3128.36	5.58E-38	1.734E-34
21	2780.76	1.48E-40	4.084E-37
22	2433.17	3.32E-43	8.034E-40
23	0	6.25E-46	0.000E+00
24	0	9.66E-49	0.000E+00
25	0	1.19E-51	0.000E+00
26	0	1.14E-54	0.000E+00
27	0	7.81E-58	0.000E+00
28	0	3.45E-61	0.000E+00
29	0	7.35E-65	0.000E+00
P_{ideal_S}/T_0			9956.77
$P_{expected_S}/T_0$			10080.27

Table 5. COPT of inverters

N_{fi}	Ideal Power (W)	Probability	Expected Power (W)
0	519037.1249	1.98E-01	1.02E+05
1	509055.6418	3.26E-01	1.64E+05
2	499074.1586	2.63E-01	1.29E+05
3	489092.6754	1.38E-01	6.68E+04
4	479111.1923	5.35E-02	2.53E+04
5	469129.7091	1.62E-02	7.52E+03
6	459148.2259	4.01E-03	1.82E+03
7	449166.7427	8.33E-04	3.70E+02
8	439185.2596	1.48E-04	6.42E+01
9	429203.7764	2.29E-05	9.69E+00
10	419222.2932	3.11E-06	1.29E+00

11	409240.81	3.75E-07	1.51E-01
12	399259.3269	4.04E-08	1.59E-02
13	389277.8437	3.93E-09	1.51E-03
14	379296.3605	3.46E-10	1.30E-04
15	369314.8774	2.77E-11	1.01E-05
16	359333.3942	2.02E-12	7.18E-07
17	349351.911	1.35E-13	4.67E-08
18	339370.4278	8.31E-15	2.78E-09
19	329388.9447	4.70E-16	1.53E-10
20	319407.4615	2.45E-17	7.72E-12
21	309425.9783	1.18E-18	3.60E-13
22	299444.4952	5.24E-20	1.55E-14
23	289463.012	2.16E-21	6.18E-16
24	279481.5288	8.25E-23	2.28E-17
25	269500.0456	2.92E-24	7.77E-19
26	259518.5625	9.57E-26	2.45E-20
27	249537.0793	2.91E-27	7.18E-22
28	239555.5961	8.21E-29	1.94E-23
29	229574.113	2.15E-30	4.87E-25
30	219592.6298	5.20E-32	1.13E-26
31	209611.1466	1.17E-33	2.41E-28
32	199629.6634	2.42E-35	4.76E-30
33	189648.1803	4.63E-37	8.66E-32
34	179666.6971	8.16E-39	1.45E-33
35	169685.2139	1.33E-40	2.22E-35
36	159703.7308	1.98E-42	3.12E-37
37	149722.2476	2.70E-44	4.00E-39
38	139740.7644	3.37E-46	4.65E-41
39	129759.2812	3.82E-48	4.90E-43
40	119777.7981	3.92E-50	4.64E-45
41	109796.3149	3.63E-52	3.93E-47
42	99814.8317	3.00E-54	2.96E-49
43	89833.3486	2.20E-56	1.96E-51
44	79851.8654	1.42E-58	1.12E-53
45	69870.3822	8.00E-61	5.52E-56
46	59888.899	3.85E-63	2.27E-58
47	49907.4159	1.55E-65	7.64E-61
48	39925.9327	5.10E-68	2.01E-63
49	29944.4495	1.32E-70	3.89E-66
50	19962.9663	2.49E-73	4.92E-69
51	9981.4832	3.09E-76	3.05E-72
52	0	1.88E-79	0.00E+00
P_{ideal_I}/T_0			9956.77
$P_{expected_I}/T_0$			10080.27

Table 6. COPT of transformers

N_{ft}	Ideal Power (W)	Probability	Expected Power (W)
0	519037.1249	1.00E+00	4.97E+05
1	519037.1249	3.22E-09	1.60E-03
2	500000	3.90E-18	1.94E-12
3	250000	2.09E-27	5.23E-22
4	0	4.22E-37	0.00E+00
P_{ideal_T}/T_0			9956.77
$P_{expected_T}/T_0$			10080.27

6. Discussion

In the literature, different methods for determining system reliability can be found. Furthermore, in this study, good system availability was observed. The literature also reports varying levels of reliability due to the fact that different topologies were analyzed in other works.

In this study, the string topology was analyzed, which is among the most reliable, presenting greater robustness against component failures, since the loss of an inverter or module affects only part of the total generation. Compared to other studies, absolute irradiance from the Arequipa region was used as a reference, while in other works, this variable is only estimated. This contributes to improved analysis performance and is directly reflected in the obtained availability index, Ae = 0.9573.

The reliability and availability values found in this study are similar to those reported in previous research. This result confirms the efficiency of the string topology and demonstrates that the use of real irradiance data increases the accuracy of the probabilistic model.

7. Conclusion

The reliability analysis of the Arequipa region showed a high availability level for a 1 MWp photovoltaic power plant. The implementation of failure and repair rates obtained from the literature allows for a more realistic assessment, since, when combined with the analysis of local irradiance, they provide results that better reflect real operating conditions. The following indices were obtained: ISE = 2,277.02 MWh, ESE = 2,179.95 MWh, and Ae = 0.9573. This indicates that approximately 95.73% of the energy that could have been generated under ideal conditions was effectively delivered to the grid. These results demonstrate the robustness of the string topology against component failures and confirm the high reliability of the system. The proposed methodology enables the reliability analysis of individual subsystems, allowing the identification of equipment with higher failure incidence and supporting studies applicable to future photovoltaic projects.

Acknowledgment

The authors gratefully acknowledge the Universidad Nacional de San Agustín de Arequipa (UNSA) for support and collaboration throughout this research.

References

[1] A. Sayed et al., "Reliability, Availability and Maintainability Analysis for Grid-Connected Solar Photovoltaic Systems," *Energies*, vol. 12, no. 7, pp. 1-18, 2019. [CrossRef] [Google Scholar] [Publisher Link]

[2] N. Unnikrishnan Nair, P.G. Sankaran, and N. Balakrishnan, *Chapter 1-Reliability Theory*, Reliability Modelling and Analysis in Discrete Time, Academic Press, pp. 1-42, 2018. [CrossRef] [Publisher Link]

[3] Smriti Singh, R.K. Saket, and Baseem Khan, "A Comprehensive Review of Reliability Assessment Methodologies for Grid-Connected Photovoltaic Systems," *IET Renewable Power Generation*, vol. 17, no. 7, pp. 1859-1880, 2023. [CrossRef] [Google Scholar] [Publisher Link]

[4] Ahmad Zaki Abdul Karim, Mohamad Shaiful Osman, and Mohd. Khairil Rahmat, "A Review on Risk and Reliability Analysis in Photovoltaic Power Generation," *Energies*, vol. 18, no. 14, pp. 1-22, 2025. [CrossRef] [Google Scholar] [Publisher Link]

[5] Amir Ahad, Noradin Ghadimi, and Davar Mirabbasi, "Reliability Assessment for Components of Large Scale Photovoltaic Systems," *Journal of Power Sources*, vol. 264, pp. 211-219, 2014. [CrossRef] [Google Scholar] [Publisher Link]

[6] Peng Zhang et al., "Reliability Assessment of Photovoltaic Power Systems: Review of Current Status and Future Perspectives," *Applied Energy*, vol. 104, pp. 822-833, 2013 [CrossRef] [Google Scholar] [Publisher Link]

[7] Giovanni Petrone et al., "Reliability Issues in Photovoltaic Power Processing Systems," *IEEE Transactions on Industrial Electronics*, vol. 55, no. 7, pp. 2569-2580, 2008. [CrossRef] [Google Scholar] [Publisher Link]

[8] Ahmed M. Mustafa et al., "Reliability Assessment of Grid Connected Photovoltaic Generation Systems," *2015 International Conference on Renewable Energy Research and Applications (ICRERA)*, Palermo, Italy, pp. 1543-1549, 2015. [CrossRef] [Google Scholar] [Publisher Link]

[9] Daniella Cohen, and David Elmakis, "Reliability of Photo-Voltaic Power Plants," *Electric Power Systems Research*, vol. 224, 2023. [CrossRef] [Google Scholar] [Publisher Link]

[10] Simona-Vasilica Oprea et al., "Photovoltaic Power Plants (PV-PP) Reliability Indicators for Improving Operation and Maintenance Activities. A Case Study of PV-PP Agigea Located in Romania," *IEEE Access*, vol. 7, pp. 39142-39157, 2019. [CrossRef] [Google Scholar] [Publisher Link]

[11] Stefan Baschel et al., "Impact of Component Reliability on Large Scale Photovoltaic Systems' Performance," *Energies*, vol. 11, no. 6, pp. 1-16, 2018 [CrossRef] [Google Scholar] [Publisher Link]

[12] Samer Sulaeman, Mohammed Benidris, and Joydeep Mitra, "Modeling and Assessment of PV Solar Plants for Composite System Reliability Considering Radiation Variability and Component Availability," *2016 Power Systems Computation Conference (PSCC)*, Genoa, Italy, pp. 1-8, 2016. [CrossRef] [Google Scholar] [Publisher Link]

[13] Dharani Kolantla et al., "Critical Review on Various Inverter Topologies for PV System Architectures," *IET Renewable Power Generation*, vol. 14, no. 17, pp. 3418-3438, 2020. [CrossRef] [Google Scholar] [Publisher Link]

[14] Susanna S. Epp, *Discrete Mathematics with Applications*, 5th ed., Cengage Learning India Pvt. Ltd, 2021. [Google Scholar] [Publisher Link]

[15] PVGIS-Photovoltaic Geographical Information System, JRC, European Commission, 2025. [Online]. Available: https://re.jrc.ec.europa.eu/pvg_tools/en/#MR

[16] Amir Ghaedi et al., "Reliability Evaluation of a Composite Power System Containing Wind and Solar Generation," *2013 IEEE 7th International Power Engineering and Optimization Conference (PEOCO)*, Langkawi, Malaysia, pp. 483-488, 2013. [CrossRef] [Google Scholar] [Publisher Link]

[17] Alessandra Colli, "Failure Mode and Effect Analysis for Photovoltaic Systems," *Renewable and Sustainable Energy Reviews*, vol. 50, pp. 804-809, 2015. [CrossRef] [Google Scholar] [Publisher Link]

[18] Marios Theristis, and Ioannis A. Papazoglou, "Markovian Reliability Analysis of Standalone Photovoltaic Systems Incorporating Repairs," *IEEE Journal of Photovoltaics*, vol. 4, no. 1, pp. 414-422, 2014. [CrossRef] [Google Scholar] [Publisher Link]

[19] Loredana Cristaldi et al., "Markov Process Reliability Model for Photovoltaic Module Encapsulation Failures," *2015 International Conference on Renewable Energy Research and Applications (ICRERA)*, Palermo, Italy, pp. 203-208, 2015. [CrossRef] [Google Scholar] [Publisher Link]

[20] Michael Perdue, and Ralph Gottschalg, "Energy Yields of Small Grid Connected Photovoltaic System: Effects of Component Reliability and Maintenance," *IET Renewable Power Generation*, vol. 9, no. 5, pp. 432-437, 2015. [CrossRef] [Google Scholar] [Publisher Link]

[21] Amir Ahadi, Hosein Hayati, and Seyed Mohsen Miryousefi Aval, "Reliability Evaluation of Future Photovoltaic Systems with Smart Operation Strategy," *Frontiers in Energy*, vol. 10, pp. 125-135, 2016. [CrossRef] [Google Scholar] [Publisher Link]